Modeling and optimization of a photovoltaic module's parameters

Mabrouk Oumayma, Abdérafi Charki, Chatti Nizar, Xavier Sidambarompoulé, Sid-Ali Blaifi

Modeling and optimization of a photovoltaic module's parameters

Oumayma Mabrouk[1,*], *Abderafi* Charki[1,**], *Nizar* Chatti[1,***], *Xavier* Sidambarompoule[1,****], and *Sid-ali* Blaifi[2,†]

[1]Angevin Research Laboratory in Systems Engineering LARIS, University of Angers, Angers, France
[2]Research Laboratory of Electrical Engineering and Automatic LREA, University of Medea, Medea, Algeria

Abstract. This study addresses the identification and optimization of parameters in the single-diode photovoltaic (PV) model (SDM), a widely adopted approach for simulating the electrical behavior of PV modules. The five key parameters, namely, the photo-generated current (I_{ph}), the reverse saturation current (I_0), the series resistance (R_s), the shunt resistance (R_{sh}), and the diode ideality factor (n), were initially estimated under Standard Test Conditions (STC) using manufacturer-provided data and the PV System toolbox in MATLAB. Based on these initial values, simulations of the current–voltage (I–V) and power–voltage (P–V) characteristics were conducted under real operating conditions using the Lambert W function and the Newton–Raphson method. An optimization procedure was then applied, combining the Newton–Raphson technique with two optimization algorithms: the Genetic Algorithm (GA) and the Levenberg–Marquardt (LM) method. The performance of each method was evaluated using three statistical indicators: Root Mean Square Error (RMSE), Mean Absolute Error (MAE), and the coefficient of determination (R^2). Among the tested approaches, the Genetic Algorithm achieved the highest accuracy, with an RMSE of 0.0359 A, a MAE of 0.0270 A, and an R^2 value of 0.9993. Finally, the analysis of environmental influence confirmed the significant impact of temperature and irradiance on module performance, particularly on the open-circuit voltage, maximum power output, and overall energy generation.

1 Introduction

In a global context marked by the energy transition and the fight against climate change, PV systems are playing an increasingly important role in the energy mix [1]. Thanks to their ability to directly convert solar energy into electricity, they offer a sustainable, clean, and renewable solution to meet the growing energy demand.

The performance of photovoltaic modules strongly depends on environmental conditions, particularly solar irradiance and temperature [2]. These parameters significantly affect the electrical characteristics of solar cells, such as short-circuit current (I_{sc}), open-circuit voltage (V_{oc}), and maximum power point (MPP). Therefore, accurate modeling of the electrical behavior of PV modules is essential for optimizing their efficiency, predicting their performance, and designing power generation systems.

In this context, the present study focuses on the electrical modeling of a monocrystalline photovoltaic module based on SANYO technology, using experimental data extracted from the literature [3]. The electrical parameters under standard test conditions (STC) were partially obtained from the manufacturer's datasheet and subsequently completed using the the MATLAB PV System toolbox.

The primary objective of this research is twofold: (i) rigorously identify the five intrinsic parameters of the SDM (I_{ph}, I_0, R_s, R_{sh}, and n); (ii) accurately simulate current-voltage (I–V) and power-voltage (P–V) curves under different operating conditions using a combination of analytical approaches and optimization algorithms. Among the methods used, the Lambert W function and the Newton–Raphson method allow inversion of the model's nonlinear equations, while GA and LM ensure robust parameter optimization.

Furthermore, this study offers a comparative evaluation of the performance of different parameter extraction methods [4] using standard statistical indicators such as RMSE, MAE, and R², along with a detailed analysis of the influence of temperature and irradiance on the electrical behavior of the PV module. These considerations are essential to ensure a realistic modeling approach that reflects actual operating conditions and meets the accuracy requirements of industrial applications and advanced research.

The structure of this paper is organized into four main sections. Section 2 presents the theoretical framework and numerical methods used for modeling and parameter identification of the single-diode model. Section 3 discusses the results obtained, emphasizing the accuracy of the different approaches and the impact of environmental conditions. Finally, Section 4 provides a summary of the main conclusions and suggests avenues for future research and development.

*e-mail: oumayma.mabrouk@univ-angers.fr
**e-mail: abderafi.charki@univ-angers.fr
***e-mail: nizar.chatti@univ-angers.fr
****e-mail: xavier.sidambarompoule@univ-angers.fr
†e-mail: s.blaifi@univ-dbkm.dz

2 Modeling and parameter optimization approach

Accurate modeling of PV modules is essential for performance prediction and system optimization. Among the various approaches available, two principal categories are generally distinguished: empirical models based on statistical or experimental correlations, and circuit-based models derived from the physical and electrical behavior of solar cells. In this work, emphasis is placed on the latter, specifically on SDM, which provides a suitable trade-off between accuracy and computational complexity.

2.1 Mathematical formulation of the Single-Diode model

The SDM is widely used to describe the current–voltage (*I–V*) behavior of solar cells, owing to its balance between accuracy and simplicity. The equivalent circuit of this model, shown in Figure 1, includes a current source I_{ph}, a diode with reverse saturation current I_0, a series resistance R_s, and a parallel (shunt) resistance R_{sh}.

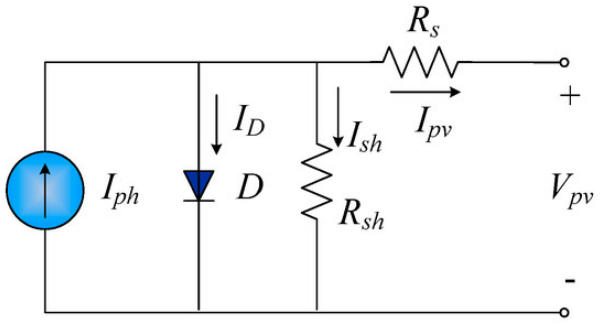

Figure 1: Single diode model (SDM)[3]

In practical configurations, a PV module consists of multiple solar cells connected in series to achieve the desired voltage level. In this study, we consider a module comprising N_s series-connected cells.
The electrical behavior of the module is represented by the Single Diode Model (SDM), as given in Equation (1), with all associated parameters and variables provided in Table 1.

$$I_{pv} = I_{ph} - I_d - I_{sh} \tag{1}$$

where

$$I_{sh} = \frac{V_{pv} + R_s I_{pv}}{R_{sh}} \tag{2}$$

and

$$I_d = I_0 \left[\exp\left(\frac{q(V_{pv} + R_s I_{pv})}{nKT} \right) - 1 \right] \tag{3}$$

The saturation current I_0 [5] is expressed as a function of temperature as follows:

$$I_0 = I_{0,\text{ref}} \left(\frac{T}{T_{\text{ref}}} \right)^3 \exp\left(\frac{E_g}{K} \left(\frac{1}{T_{\text{ref}}} - \frac{1}{T} \right) \right) \tag{4}$$

Thus, for a single cell, the characteristic equation becomes:

$$I_{pv} = I_{ph} - I_0 \left[\exp\left(\frac{q\left(V_{pv} + I_{pv}R_s\right)}{nkT} \right) - 1 \right] - \left(\frac{V_{pv} + I_{pv}R_s}{R_{sh}} \right) = f\left(I_{ph}, V_{pv}, \theta\right) \tag{5}$$

Where θ is the vector of the five intrinsic parameters I_{ph}, I_0, R_s, R_{sh}, and n.

Table 1: Parameters of the SDM model

Symbol	Description
I_{pv}	Photovoltaic current (A)
I_{ph}	Photocurrent (A)
I_0	Diode saturation current (A)
$I_{0,\text{ref}}$	Diode saturation current at STC (A)
V_{pv}	Photovoltaic voltage (V)
R_s	Series resistance (Ω)
R_{sh}	Shunt (parallel) resistance (Ω)
n	Diode ideality factor
q	Elementary charge (1.602×10^{-19} C)
K	Boltzmann constant (1.38×10^{-23} J/K)
E_g	Band gap energy
T	Temperature in Kelvin (K)
T_{ref}	Temperature at STC (25 °C = 298.15 K)
G	Irradiance (W/m^2)
N_s	Number of cells in series
STC	Standard Test Conditions (T = 25 °C, G = 1000 W/m^2)

This model depends on five intrinsic parameters that must be accurately estimated: the photo-generated current I_{ph}, the reverse saturation current I_0, the series resistance R_s, the shunt resistance R_{sh}, and the diode ideality factor n. The precision with which these parameters are determined directly affects the model's ability to replicate the actual electrical behavior of the photovoltaic module.

To support the parameter extraction process, three characteristic points of the I–V curve are commonly used:

- Open-circuit voltage (V_{oc}), corresponding to the maximum voltage when the output current is zero (I=0);
- Short-circuit current (I_{sc}), representing the maximum current when the output voltage is zero (V=0);
- Maximum Power Point (MPP), defined by the pair (V_{mp},I_{mp}), which corresponds to the operating condition where the product $V_{\text{mp}} \times I_{\text{mp}}$ reaches its maximum.

These points serve as essential reference values in the parameter identification process, ensuring that the simulated I–V and P–V characteristics closely match the experimental measurements.

2.2 Numerical techniques for parameter extraction and optimization

To determine the SDM parameters, several numerical methods are employed. These methods minimize the deviation between experimental I–V curves and those predicted by the model. The techniques used in this study are: the Lambert W function for analytical inversion, the Newton–Raphson method for iterative solving, and two optimization algorithms: Genetic Algorithm (GA) and Levenberg–Marquardt (LM).

2.2.1 The Lambert W method

The Lambert W method [6] is based on the use of the $W(z)$ function, defined as the solution of the equation:

$$W(z)e^{W(z)} = z$$

This function enables the transformation of nonlinear equations containing expressions of the form ze^z into a tractable analytical form.

In the context of the single-diode photovoltaic model, the relationship between the current I_{pv} and the voltage V_{pv} can be expressed using the Lambert W function. The dependence of the current I_{pv} on the five PV model parameters (I_{ph}, I_0, n, R_s, and R_{sh}) can thus be explicitly determined.

The reformulated expression, which uses the Lambert W function, is given by:

$$I_{pv} = \frac{R_{sh}(I_{ph} + I_0) - V_{pv}}{R_{sh} + R_s} - \frac{nKT}{qR_s} W\left[\frac{qR_s I_0 R_{sh}}{nKT(R_{sh} + R_s)} \times \exp\left(\frac{q}{nKT}\frac{R_{sh}(R_s(I_{ph} + I_0) + V_{pv})}{R_{sh} + R_s}\right)\right] \quad (6)$$

The use of the Lambert W function in this reformulation makes the dependence of the current I_{pv} on the five PV model parameters explicitly clear.

2.2.2 Newton-Raphson method

Newton-Raphson method [7] is an iterative numerical technique used to solve nonlinear equations, particularly well-suited for single-diode photovoltaic modeling. This approach successively updates current approximations (I_{pv}) using the formula:

$$I_{n+1} = I_n - \frac{f(I_n)}{f'(I_n)} \quad (7)$$

where $f(I_n)$ is the implicit current expression, as defined in Equation (5), and $f'(I_n)$ is its derivative with respect to current.

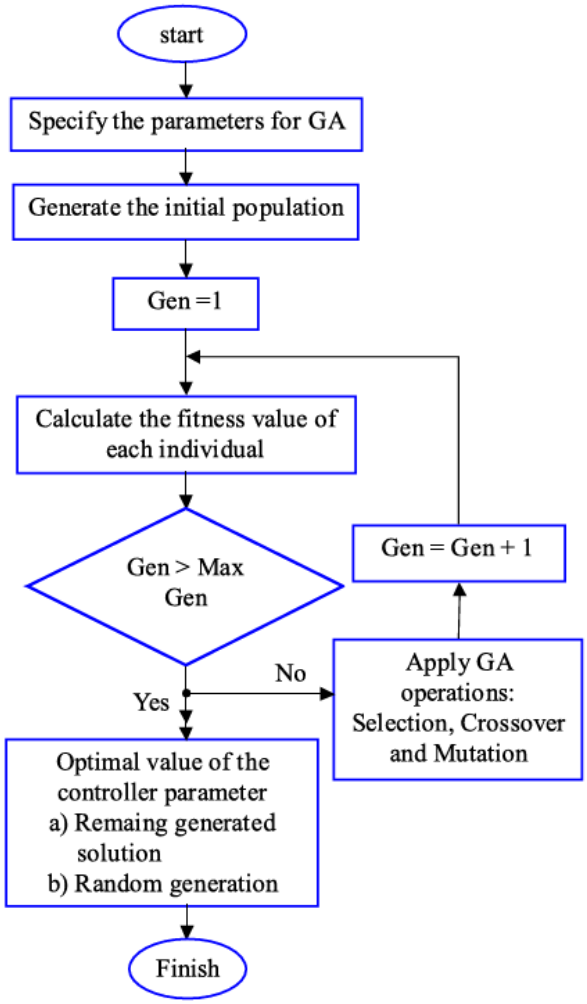

Figure 2: Flowchart of the genetic algorithm [8]

2.2.3 The Genetic Algorithm (GA)

The Genetic Algorithm (GA) [8] is a stochastic optimization method inspired by the mechanisms of natural evolution. It is particularly well-suited for solving nonlinear and multidimensional problems.

The algorithm begins with the specification of GA parameters (population size, mutation rate, etc.), followed by the generation of an initial random population of solutions. Each individual is then evaluated using a fitness function, often based on the error between experimental and simulated data. In each generation, the GA applies selection, crossover, and mutation operations to produce new individuals. This iterative process is repeated until a maximum number of generations is reached. If this criterion is satisfied, the optimal solution is selected from among the generated individuals. The flowchart in Figure 2 also highlights two finalization strategies: reusing the best solutions or generating complementary random solutions, depending on the case.

2.2.4 The Levenberg-Marquardt (LM) algorithm

LM [9] is a nonlinear optimization method that combines the advantages of both the least squares and the gradient descent approaches.

The smooth transition between these two behaviors is managed by a control parameter called the damping factor λ. This parameter adjusts the trade-off between the two approaches:

- When λ is large, the Levenberg–Marquardt algorithm behaves like gradient descent (more robust but slower).
- When λ is small, it behaves like Gauss–Newton (faster but more sensitive to errors).

At each i^{th} iteration, the following system is solved:

$$\left(\mathbf{J}^T\mathbf{J} + \lambda_i\mathbf{I}\right)\Delta\boldsymbol{\theta} = \mathbf{J}^T\boldsymbol{\varepsilon} \tag{8}$$

where $\boldsymbol{\varepsilon} = I_{\text{sim},i} - I_{\text{meas},i}$,
$\Delta\boldsymbol{\theta} = \boldsymbol{\theta}_{i+1} - \boldsymbol{\theta}_i$,
$\boldsymbol{\theta}$ is the parameter vector,
$\mathbf{I}$ is the identity matrix, λ_i is the damping factor (adapted at each iteration), and
$\mathbf{J}$ is the Jacobian matrix, which contains the partial derivatives of the residual function f with respect to each parameter in the vector $\boldsymbol{\theta}$.

Based on the modeling framework and estimation techniques outlined above, the present section investigates the performance of the single-diode model using different parameter extraction methods. The accuracy of each approach is assessed by comparing the simulated I–V and P–V characteristics against experimental data, and the influence of temperature and irradiance is also examined.

3 Results and discussion

3.1 Evaluation metrics and selection criteria

To evaluate the performance of the parameter extraction methods, the simulated current–voltage (I–V) and power–voltage (P–V) characteristics are compared to experimental measurements using standard statistical indicators. Three main error metrics are considered in this study.

The Root Mean Square Error (RMSE) provides a global measure of the deviation between the simulated and measured current values, giving greater weight to larger errors:

$$RMSE = \sqrt{\frac{1}{N}\sum_{i=1}^{N}(I_{sim,i} - I_{meas,i})^2} \tag{9}$$

where $I_{sim,i}$ and $I_{meas,i}$ represent the simulated and measured current values, respectively, and N is the number of data points.

The Mean Absolute Error (MAE) reflects the average magnitude of individual errors, offering a more intuitive interpretation of the discrepancy between simulated and observed data:

$$MAE = \frac{1}{N}\sum_{i=1}^{N}|I_{sim,i} - I_{meas,i}| \tag{10}$$

The coefficient of determination (R^2) quantifies the quality of the fit by indicating the proportion of variance in the measured data that is explained by the model:

$$R^2 = 1 - \frac{\sum_{i=1}^{N}(I_{meas,i} - I_{sim,i})^2}{\sum_{i=1}^{N}(I_{meas,i} - \overline{I_{meas}})^2} \tag{11}$$

where $\overline{I_{meas}}$ is the mean of the measured current values.

Although the Mean Absolute Percentage Error (MAPE) is commonly used in photovoltaic modeling:

$$MAPE = \frac{100}{N}\sum_{i=1}^{N}\left|\frac{I_{sim,i} - I_{meas,i}}{I_{meas,i}}\right| \tag{12}$$

it is not retained in this study due to its tendency to yield distorted results when current values approach zero, as demonstrated in Table 2.

These indicators offer complementary perspectives for assessing the accuracy and reliability of each algorithm in reproducing the real electrical behavior of the PV module.

3.2 Implementation of parameter extraction algorithms

The dataset used in this study is extracted from the article *"An enhanced dynamic modeling of PV module using Levenberg-Marquardt algorithm"* written by Blaifi [3]. The nominal electrical parameters under Standard Test Conditions (STC) were partially provided by the manufacturer, as detailed in Table 3.

To estimate the remaining intrinsic parameters namely, the series resistance R_s, shunt resistance R_{sh}, diode ideality factor n, reverse saturation current I_0, and photogenerated current I_{pv}, the PV Array block from the Simscape Electrical library in MATLAB/Simulink was used.

This modeling block is based on the classical single-diode equivalent circuit, which accurately reproduces the current–voltage (I-V) characteristics of photovoltaic modules. It also incorporates the influence of temperature and irradiance on the module's electrical performance. As part of the Simscape environment, it enables the simulation of multidomain physical systems, thereby allowing for integrated and flexible modeling workflows.

The PV Array block requires the following standard input data under STC:

- Maximum power P_{max},
- Voltage and current at the maximum power point: V_{mp}, I_{mp},
- Open-circuit voltage V_{oc},
- Short-circuit current I_{sc},
- Number of series and parallel cells.

From these inputs, the block automatically estimates the internal parameters of the single-diode model: R_s, R_{sh}, n, I_0, and I_{pv}. This feature makes it an effective tool for initializing or validating analytical PV models.

Table 2: Example illustrating the limitation of MAPE with small measured values

Actual Value (A)	Predicted Value (A)	Absolute Error (A)	Relative Error (%)
0.01	0.02	0.01	100%
5.00	5.05	0.05	1%

Table 3: Technical specifications of the SANYO monocrystalline module [3]

Description	Value
Number of cells	96
Cell type	Monocrystalline
Cell dimensions	156 x 156 mm
PV module dimensions	1319 x 894 x 35 mm
Nominal power	180 W
Open-circuit voltage (V_{OC})	66.4 V
Short-circuit current (I_{SC})	3.65 A
Voltage at MPP (V_{mpp})	54 V
Current at MPP (I_{mpp})	3.33 A
Nominal operating temperature (NOCT)	45 ± 2 °C
Temperature coefficient (P_{max})	−0.33 % °C^{-1}
Temperature coefficient (I_{SC})	1.10 mA/°C
Temperature coefficient (V_{OC})	−0.173 V/°C

The experimental data corresponds to a photovoltaic module operating under real-world conditions, with: Cell temperature $T = 47.84\,°C$ and Irradiance $G = 766.04\,W/m^2$.

Initially, STC parameters were used as a baseline for extracting the simulated curves $I_{\text{sim}}(V)$ and $P_{\text{sim}}(V)$ using the Lambert W and Newton-Raphson methods, allowing for an initial comparison with the experimental curves. Parameter optimization was then carried out using the GA and LM algorithms, applied to the Newton-Raphson method. Each method was evaluated based on performance metrics. This process is illustrated in Figure 3.

The results are summarized in Table 4.

3.3 Effectiveness of genetic algorithm in model fitting

As shown in Table 4, the use of an optimizer is essential to accurately extract the parameters of the single-diode model. Among the two methods evaluated, the Genetic Algorithm (GA) clearly demonstrates superior performance. These results confirm the robustness of GA when dealing with the nonlinear and highly multimodal nature of the optimization problem.

Figure 4 illustrates the evolution of the fitness value across generations. A rapid improvement is observed during the initial iterations, followed by a gradual convergence toward a stable minimum. This convergence

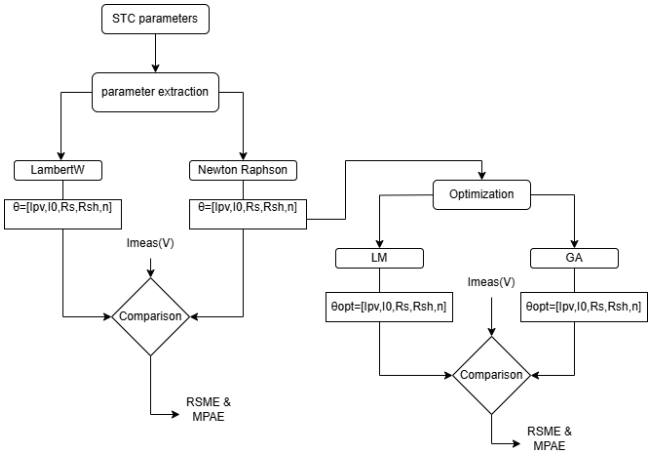

Figure 3: Flowchart of photovoltaic parameter extraction and optimization methodology

behavior demonstrates the GA's effectiveness in exploring the search space while avoiding local minima due to its stochastic operators.

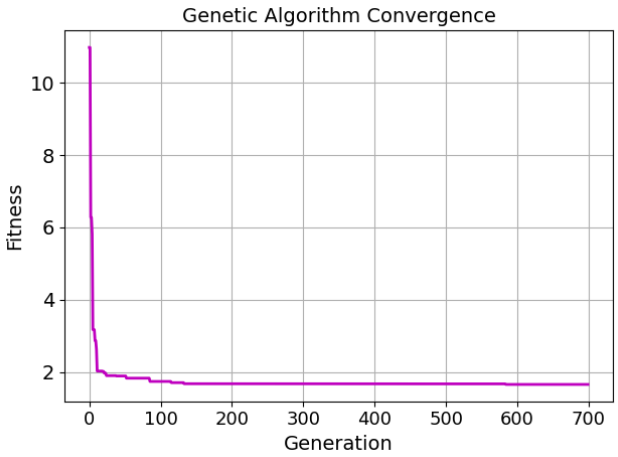

Figure 4: GA convergence

Finally, Figure 5 provides a visual comparison between the experimental I–V curves, the curves generated using parameters extracted by the Newton-Raphson method, and those obtained after GA based optimization. The latter shows a noticeably better match with the measured data, confirming the improved accuracy achieved through the GA approach.

After numerous iterations to achieve optimal fitness and performance metrics, the Genetic Algorithm (GA) was

Table 4: Comparison of optimization methods for PV parameter extraction

	LambertW	**Newton-Raphson**	**NewtonR+GA**	**NewtonR+LM**
RMSE I-V (A)	0.3409	0.1852	0.0359	0.041
MAE I-V (A)	0.3278	0.1566	0.0270	0.04
R^2	0.9354	0.9809	0.9993	0.9981

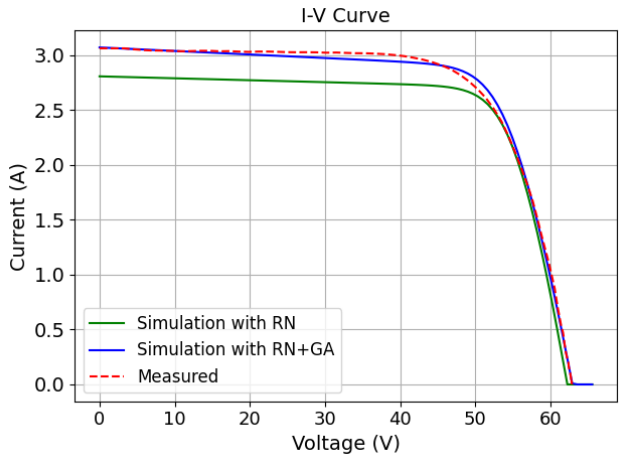

Figure 5: I-V Curve with GA optimisation

configured with the set of hyperparameters presented in Table 5.

Table 5: Genetic algorithm (GA) hyperparameters

Hyperparameter	**Value**
Population size	100
Generations	700
Crossover fraction	0.5
Mutation rate	0.1

3.4 Impact of environmental conditions on module behavior

Environmental factors, particularly temperature T and irradiance G, have a significant impact on the electrical behavior of photovoltaic modules (PV). Using our optimized SDM, we analyzed the variation of the key parameters I_{pv}, n, R_s, and R_{sh} under changing temperature and irradiance conditions.

3.4.1 Sensitivity analysis of SDM parameters to temperature and irradiance

The analysis of the Single Diode Model (SDM) parameters under varying environmental conditions has provided valuable insights into the behavior of photovoltaic modules. Each of the key parameters I_{pv}, n, Rs, and R_{sh} exhibits distinct sensitivity to changes in temperature and irradiance.

The photogenerated current (I_{pv}) demonstrates a linear increase with irradiance and a moderate rise with temperature. This is consistent with the physical principle that a higher photon flux generates more charge carriers. As shown in Figure 6, I_{pv} rises proportionally with G at a fixed temperature of 30°C, confirming its strong dependence on irradiance. The shunt resistance (R_{sh}) is highly

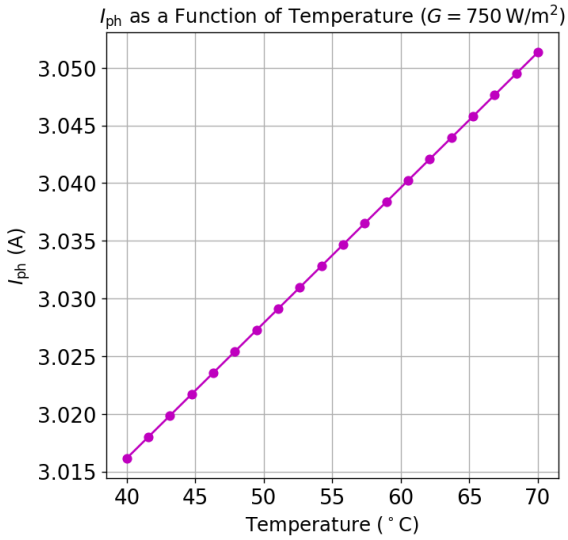

(a)

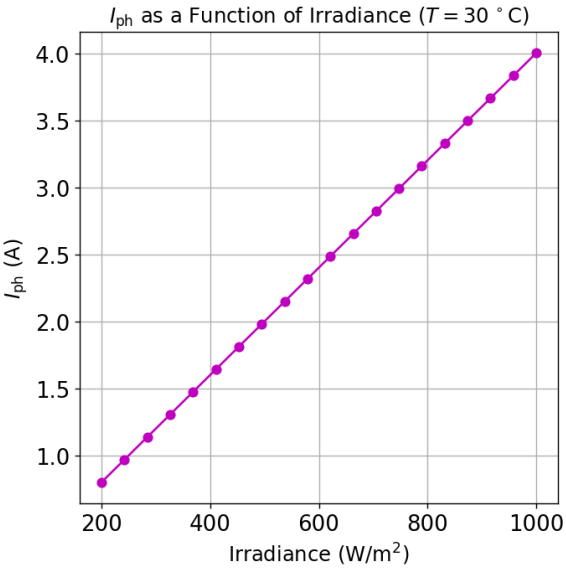

(b)

Figure 6: Variation of photogenerated current I_{ph} with (a) temperature and (b) irradiance

sensitive to irradiance, displaying a notable decrease as G increases, while remaining almost insensitive to temperature changes. This behavior is evident in Figure 7, where R_{sh} is plotted as a function of irradiance at a fixed temperature.

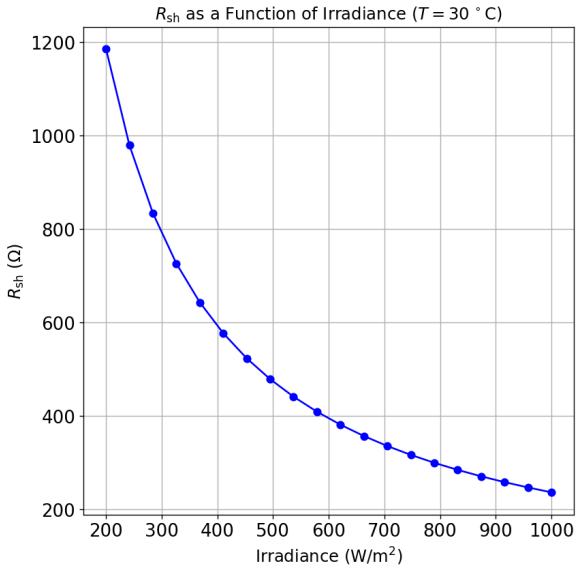

Figure 7: Variation of R_{sh} with irradiance

Both the n and the R_s remain relatively stable across variations in T and G. These parameters exhibit only slight fluctuations and can thus be reasonably approximated as constants for most simulation and modeling tasks. This stability simplifies the parameter identification process and reduces model complexity.

3.4.2 *Influence of irradiance on I-V curve and P-V curve*

Irradiance and temperature have a significant impact on the electrical behavior of photovoltaic modules. By fixing the temperature at T=25°C and varying the irradiance, it is observed that an increase in irradiance leads to a proportional rise in the I_{sc}, which causes an upward shift of the I-V curves and an increase in the maximum power (P_{max}). On the other hand, the V_{oc} remains barely sensitive to irradiance, as shown in figure 8.

3.4.3 *Influence of temperature on I-V curve and P-V curve*

To analyze the temperature influence, we varied the temperature at T = 10°C, T = 25°C, and T = 50°C, while maintaining constant irradiance G at 750 W/m².

In contrast, an increase in temperature causes a significant decrease in Voc, without substantially affecting the I_{sc}. This leads to reduced maximum extractable power from the module. This thermal effect causes a leftward shift of the I–V curves and a decline in the peak of the

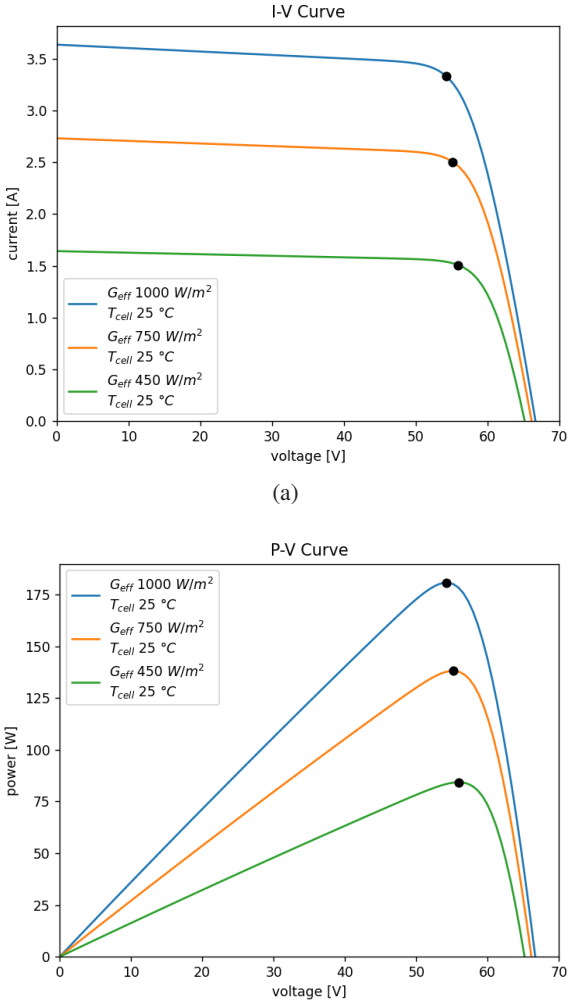

Figure 8: Influence of irradiance on the I-V curve (a) and the P-V curve (b)

P–V curve, as illustrated in Figure 9.

In summary, as shown in figure 8, an increase in G leads to an increase in I_{sc} and P_{max}. Conversely, figure 9 illustrates that an increase in T causes a decrease in V_{oc} and P_{max}.

We arbitrarily varied irradiance G and temperature T to observe their effects on I-V and P-V curves. However, literature [10] often expresses the relationship between these quantities through Equation (13):

$$T_c = T_m + \frac{G}{G_{STC}} \cdot \Delta T \tag{13}$$

Where T_c is the photovoltaic cell temperature (°C),
T_m is the measured temperature at the rear surface of the module (°C),
G is the solar irradiance on the module plane (W/m²),

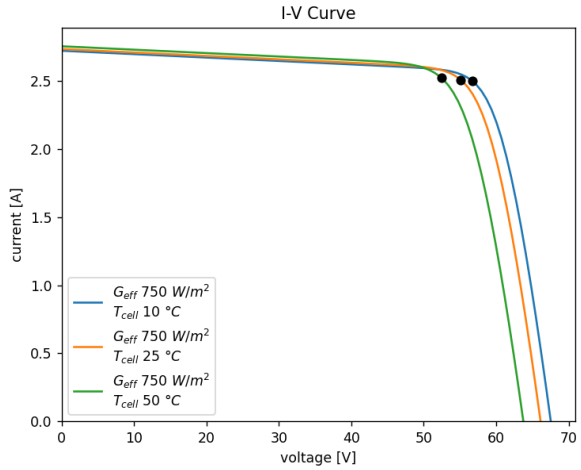

(a)

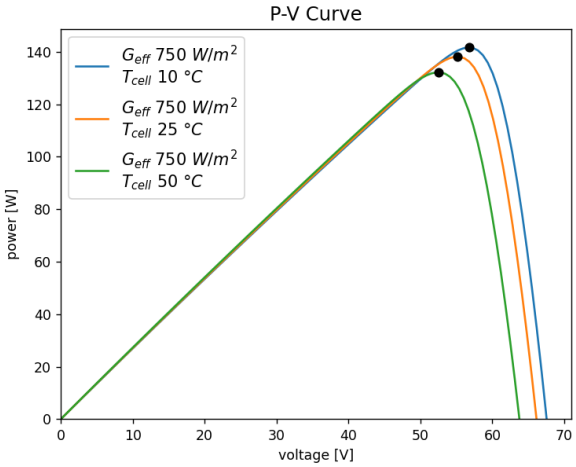

(b)

Figure 9: Influence of temperature on the I-V curve (a) and the P-V curve (b)

G_{STC} is the reference irradiance under Standard Test Conditions (1000 W/m²),
ΔT is the typical thermal difference between the cell and the module's rear surface at G = 1000 W/m² (typically 2–3°C, depending on the module technology and mounting configuration).

4 Conclusion

This study enabled the development and evaluation of a simulation model for a monocrystalline PV module, based on experimental data available in the literature. Starting from the standard single-diode model formulation, the intrinsic electrical parameters were estimated and refined using several numerical techniques, including the Newton–Raphson method, the Lambert W function, and optimization algorithms such as the Genetic Algorithm (GA) and the Levenberg–Marquardt (LM) method.

The results showed that optimization methods significantly enhance the accuracy of the model, with the Genetic Algorithm in particular achieving superior performance in terms of error minimization, as evidenced by lower RMSE and MAE values. Moreover, the influence of environmental conditions was clearly characterized: irradiance was found to have a major impact on the output current and maximum power, whereas temperature primarily affected the open-circuit voltage and led to a decrease in overall module efficiency.

In conclusion, parameter optimization under realistic operating conditions yields a more accurate representation of the dynamic behavior of PV modules. Such modeling improvements are essential for reliable performance prediction, advanced system control, and seamless integration into smart grid infrastructures.

Several avenues for future research can be identified. First, the proposed modeling approach could be extended to multi-module PV systems arranged in series or parallel configurations, particularly under rapidly changing irradiance profiles. Additionally, incorporating dynamic modeling of photovoltaic systems would allow a more accurate analysis of transient responses to environmental variations, such as shading, cloud movement, or rapid temperature changes. Furthermore, the use of more advanced models, such as the two-diode model or the Sandia performance model, may offer a more comprehensive description of the PV module's electrical behavior and enhance the fidelity of simulations under real-world operating conditions.

References

[1] IEA, *World Energy Outlook 2023* (International Energy Agency, Paris, 2023), pp. 355. https://iea.blob.core.windows.net/assets/86ede39e-4436-42d7-ba2a-edf61467e070/WorldEnergyOutlook2023.pdf

[2] Bamisile, O., Acen, C., Cai, D., Huang, Q., Staffell, I., The environmental factors affecting solar photovoltaic output. *Renewable and Sustainable Energy Reviews* **208**, 115073 (2025). https://doi.org/10.1016/j.rser.2024.115073

[3] Blaifi, S., Moulahoum, S., Taghezouit, B., Saim, A., An enhanced dynamic modeling of PV module using Levenberg-Marquardt algorithm. *Renewable Energy* **135**, 745–760 (2019). https://doi.org/10.1016/j.renene.2018.12.054

[4] Maniraj, B., Peer Fathima, A., Parameter extraction of solar photovoltaic modules using various optimization techniques: a review. *J. Phys.: Conf. Ser.* **1716**, 012001 (2020). https://iopscience.iop.org/article/10.1088/1742-6596/1716/1/012001/pdf

[5] Refdinal, N., Kiki, K., Syafii, Prima, C., Optimization active and reactive power flow for PV connected to grid system using Newton Raphson method. *Energy Procedia* **68**, 77–86 (2015). https://doi.org/10.1016/j.egypro.2015.03.235

[6] Kanimozhi, G., Kumar, H., Modeling of solar cell under different conditions by Ant Lion Optimizer with LambertW function. *Applied Soft Computing* **71**, 141–151 (2018). https://doi.org/10.1016/j.asoc.2018.06.025

[7] Chermite, C., Douiri, M. R., Hybrid Tiki Taka and Mean Differential Evolution based Weibull distribution: A comprehensive approach for solar PV modules parameter extraction with Newton-Raphson optimization. *Energy Conversion and Management* **314**, 118705 (2024). https://doi.org/10.1016/j.enconman.2024.118705

[8] Safari, A., Ahmadian, A., Aliakbar Golkar, M., Comparison of Honey Bee Mating Optimization and Genetic Algorithm for Coordinated Design of PSS and STATCOM Based on Damping of Power System Oscillation. *Journal of Electrical Engineering* **64**, 133–142 (2013). https://doi.org/10.2478/jee-2013-0020

[9] Dkhichi, F., Oukarfi, B., Fakkar, A., Belbounaguia, N., Parameter identification of solar cell model using Levenberg–Marquardt algorithm combined with simulated annealing. *Solar Energy* **110**, 781–788 (2014). https://doi.org/10.1016/j.solener.2014.09.033

[10] King, D.L., Boyson, W.E., Kratochvill, J.A., *Photovoltaic Array Performance Model* (Sandia National Laboratories, SAND2004-3535, 2004). https://www.osti.gov/servlets/purl/919131